Enhanced Fusion-Evaporation Cross Sections in Neutron-Rich ^{132}Sn on ^{64}Ni

J. F. Liang,[1] D. Shapira,[1] C. J. Gross,[1] J. R. Beene,[1] J. D. Bierman,[2] A. Galindo-Uribarri,[1] J. Gomez del Campo,[1] P. A. Hausladen,[1] Y. Larochelle,[3] W. Loveland,[4] P. E. Mueller,[1] D. Peterson,[4] D. C. Radford,[1] D.W. Stracener,[1] and R. L. Varner[1]

[1]*Physics Division, Oak Ridge National Laboratory, Oak Ridge, Tennessee 37831, USA*
[2]*Physics Department AD-51, Gonzaga University, Spokane, Washington 99258-0051, USA*
[3]*Department of Physics and Astronomy, University of Tennessee, Knoxville, Tennessee 37966, USA*
[4]*Department of Chemistry, Oregon State University, Corvallis, Oregon 97331, USA*

(Received 31 March 2003; published 8 October 2003)

Evaporation residue cross sections have been measured with neutron-rich radioactive ^{132}Sn beams on ^{64}Ni in the vicinity of the Coulomb barrier. The average beam intensity was 2×10^4 particles per second and the smallest cross section measured was less than 5 mb. Large sub-barrier fusion enhancement was observed. Coupled-channel calculations taking into account inelastic excitation significantly underpredict the measured cross sections below the barrier. The presence of several neutron transfer channels with large positive Q values suggests that multinucleon transfer may play an important role in enhancing the fusion of ^{132}Sn and ^{64}Ni.

DOI: 10.1103/PhysRevLett.91.152701 PACS numbers: 25.60.Pj, 24.10.Eq, 25.70.Jj

The interaction of two colliding nuclei consists of an attractive nuclear potential and a repulsive Coulomb potential. This creates a Coulomb barrier which the system has to overcome in order to fuse. At energies below the barrier, fusion occurs by quantum tunneling. Sub-barrier fusion cross sections for heavy ions are often found enhanced over the one-dimensional barrier penetration model (BPM) prediction. The enhancement can be explained in most cases by the coupling of the relative motion and the nuclear structure degrees of freedom of the participating nuclei [1]. It has been suggested that the fusion yield would be further enhanced when the reaction is induced by unstable neutron-rich nuclei [2–4]. This is attributed to the large N/Z ratio of these nuclei reducing the barrier height and the presence of a large number of nucleon transfer channels which can serve as doorway states to fusion [5]. Sub-barrier fusion can be used in experiments to produce superheavy elements. Using closed shell neutron-rich projectile and target will lead to compound systems with lower excitation energies and with a smaller fissility and, therefore, a higher survival probability [6].

The experimental search for fusion enhancement in heavy ion reactions has been pursued at several laboratories using neutron-rich radioactive beams. The measurements of ^{38}S + ^{181}Ta [7] and ^{29,31}Al + ^{197}Au [8] found only the enhancement expected from the lowering of the barrier height caused by the larger radii of the neutron-rich nuclei compared to the stable ^{32}S and ^{27}Al, respectively. This paper reports the first reaction study using accelerated unstable neutron-rich ^{132}Sn beams to measure fusion-evaporation cross sections. The doubly magic ^{132}Sn ($Z = 50$, $N = 82$) has eight extra neutrons compared to the heaviest stable Sn isotope, ^{124}Sn. The N/Z ratio of ^{132}Sn (1.64) is larger than that of ^{48}Ca (1.4) and ^{208}Pb (1.54) which are closed shell nuclei commonly used to produce heavy elements [9]. The target, ^{64}Ni, is semi-magic ($Z = 28$) and is the most neutron-rich stable isotope of nickel. The compound nucleus formed in this experiment, ^{196}Pt, lies in the valley of β stability. It has initial excitation energies greater than 30 MeV and can decay by particle evaporation or fission.

The experiment was carried out at the Holifield Radioactive Ion Beam Facility (HRIBF) at Oak Ridge National Laboratory. The isotope separator online technique was used to produce radioactive ^{132}Sn. Isobaric contaminants at $A = 132$ were suppressed by extracting molecular SnS^+ from the ion source and subsequently breaking it up in the charge exchange cell where the SnS^+ was converted to Sn^- [10]. The ^{132}Sn ions were postaccelerated to six energies (453, 475, 489, 504, 536, and 560 MeV) and delivered to the target. The beam intensity was measured by passing it through a 10 μg/cm^2 carbon foil and detecting the secondary electrons in a microchannel plate (MCP) detector. Three of these MCP systems were used in this experiment for monitoring the beam and providing timing signals. The average beam intensity was 2×10^4 particles per second (pps) with a maximum near 3×10^4 pps. The purity of the ^{132}Sn beam was checked by measuring the energy loss in an ionization chamber (IC). A ^{132}Te beam was used to calibrate the energy loss spectrum. It was determined that the impurity was less than 2% and that all measurable impurities had a higher atomic number (Z) than Sn. This impurity has negligible effect on the measurement because the higher Coulomb barrier suppresses the fusion of the contaminants with the target. A ^{124}Sn beam was used as a guide beam to set up the accelerator and beam line optics. At the target position, the beam was focused to a spot 1.0 mm horizontally and 2.5 mm vertically. The shape of the

 © 2003 The American Physical Society

guide beam was recorded by an electronic phosphor [11] located 74 cm in front of the target. This beam was also used for testing the detector system. The ^{132}Sn beam was then tuned by scaling the optical elements and comparing the beam shape with that of the guide beam using the electronic phosphor.

The evaporation residues (ERs) were detected along with beam particles by a timing detector and an IC located 16.9 cm from the target at 0°. They were identified by their time of flight and energy loss in the IC. The acceptance of the timing detector was a 2.54 cm diameter circle and the detection efficiency was approximately 100% for these heavy ions. In the time-of-flight measurement, the coincidence between two timing detectors placed 119 and 315 cm upstream from the target provided the timing references. The data acquisition was triggered by the scaled down beam singles or the ER-beam particle coincidences. With this triggering scheme an overall dead time of less than 5% was achieved. The IC was filled with CF_4 gas. The pressure was adjusted between 50 and 60 Torr to optimize the separation of ERs from the beam. A detailed description of the experimental apparatus will be published elsewhere [12]. Figure 1 shows the histogram of the energy loss in the first two segments of the IC for a beam energy of 536 MeV. Although there is some signal pileup introduced by directly injecting the beam into the detector, it is clear that the ERs are still well separated from the beam. With this setup, measurement of ER cross sections less than 5 mb can be achieved.

The cross section was obtained by integrating the ER yield and summing the beam particles in the IC. Because

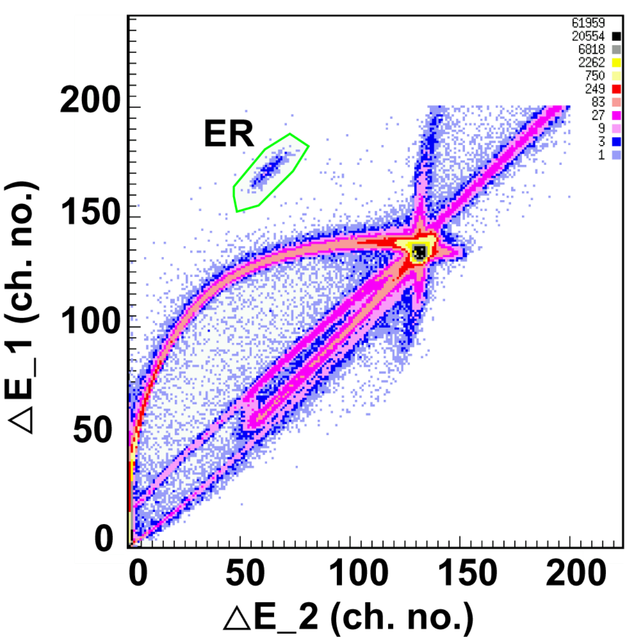

FIG. 1 (color online). Histogram of the energy loss of beam and ERs measured in the first two segments of the ionization chamber for 536 MeV ^{132}Sn + ^{64}Ni.

of the low intensity of radioactive beams, the measurement was performed with a thick target, 1 mg/cm^2 self-supporting highly enriched (99.8%) ^{64}Ni foil. The target thickness was determined by measuring the energy loss of α particles emitted from a ^{244}Cm source and a 536 MeV ^{132}Sn beam passing through the target, and by measuring the weight and area of the target. The energy loss of ^{132}Sn projectiles in the target was approximately 40 MeV. At energies below the Coulomb barrier, the excitation function falls off exponentially. For this reason, the measured cross section ($\sigma_{\rm meas}$) is sensitive predominantly to the front portion of the target and is actually a weighted average of the cross section over the range of energy loss in the target, from the energy of the beam entering the target ($E_{\rm in}$ = beam energy corrected for the energy loss in the carbon foils) to that exiting the target ($E_{\rm out}$), namely,

$$\sigma_{\rm meas} = \frac{\int_{E_{\rm in}}^{E_{\rm out}} \sigma(E) dE}{\int_{E_{\rm in}}^{E_{\rm out}} dE}. \quad (1)$$

To determine the effective reaction energy, the cross section was parametrized as an exponential function, $\sigma(E) = N \exp(\alpha E)$, where N is a normalization factor and α is a slope parameter. By solving the integral Eq. (1) for two adjacent data points in the excitation function, N and α were obtained. Subsequently, the effective energy is deduced by inverting the exponential function, namely, $E = \ln(\sigma_{\rm meas}/N)/\alpha$.

Since this experiment was performed in inverse kinematics (a heavy projectile on a light target) the ERs were very forward focused. However, the shape of the beam spot was not symmetric. Moreover, one of the disadvantages of using a thick target is the multiple scattering which results in broadening the angular distribution. Monte Carlo simulations were used to estimate the efficiency of the apparatus. The angular distribution of ERs was generated by the statistical model code PACE [13] and the width of the distribution of multiple scattering angles was predicted by Ref. [14]. The simulations show that the efficiency of the apparatus changes from 95 ± 1% for the lowest beam energy to 98 ± 1% for the highest energy.

Figure 2 presents the fusion-evaporation excitation function of ^{132}Sn + ^{64}Ni measured in this work (solid circles) and that of ^{64}Ni on even Sn isotopes measured by Freeman *et al.* [15]. The open circle is our measurement using the ^{124}Sn guide beam which is consistent with the measurement of Ref. [15] as shown by the open triangles. In Fig. 2 the energy is scaled by the fusion barrier (V_B) predicted by the Bass model [16] and the ER cross section is scaled by the size of the reactants using $R = 1.2(A_p^{1/3} + A_t^{1/3})$ fm, where A_p (A_t) is the mass of the projectile (target). It can be seen that at the highest energy the ER cross section for ^{132}Sn + ^{64}Ni is larger. This can be expected from the higher stability against fission for the neutron-rich compound nucleus.

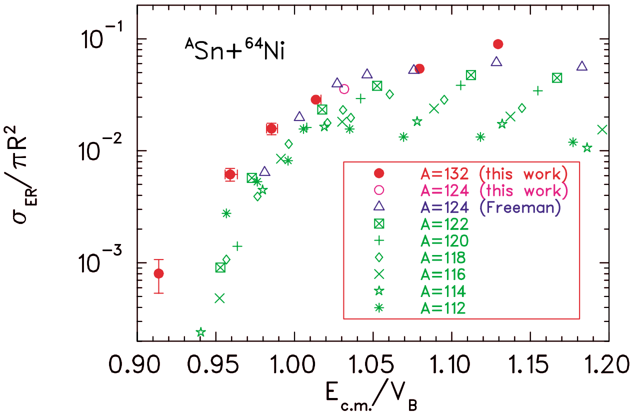

FIG. 2 (color online). Fusion-evaporation excitation functions of ^{132}Sn + ^{64}Ni (filled circles) and ^{64}Ni on even $^{112-124}$Sn [15]. The open circle is our measurement using a ^{124}Sn beam.

At energies below the barrier, the ER cross sections for ^{132}Sn + ^{64}Ni are found much enhanced comparing to those of ^{64}Ni + $^{112-124}$Sn and a simple shift of the barrier height cannot explain the enhancement.

To compare the measured excitation function with fusion models, it is necessary to estimate fission yields in the reaction. Statistical model calculations were carried out using the code PACE. The input parameters were determined by reproducing the ER and fission cross sections of ^{64}Ni + ^{124}Sn in Ref. [17]. The following parameters were used: level density parameter $a = A/8$ MeV^{-1} where A is the mass of the compound nucleus, ratio of the Fermi gas level density parameter at the saddle point to that of the ground state $a_f/a_n = 1$, diffuseness of spin distribution $d = 4\hbar$, and Sierk's fission barrier [18]. The calculations predict that fission is negligible for ^{132}Sn + ^{64}Ni and ^{64}Ni + ^{124}Sn at $E_{c.m.} \leq 160$ MeV. Therefore, the following discussion will be restricted to the data points at $E_{c.m.} \leq 160$ MeV where the ER cross sections are taken as fusion cross sections.

Large sub-barrier fusion enhancement in ^{132}Sn + ^{64}Ni can be seen when the excitation function is compared to a one-dimensional BPM shown by the dotted curve in the upper panel of Fig. 3. The nuclear potential was assumed to have a Woods-Saxon shape. The potential parameters were obtained by adjusting them to reproduce the fusion cross section of ^{64}Ni + ^{124}Sn in Ref. [17] at high energies. They are depth $V_0 = 76.6$ MeV, radius parameter $r_0 =$ 1.2 fm, and diffuseness parameter $a = 0.65$ fm.

It is well established that sub-barrier fusion enhancement can be described by channel couplings [1]. The couplings result in splitting the single barrier into a distribution of barriers. The incident flux overcoming the low energy barriers gives rise to the enhanced fusion cross sections [19–21]. Coupled-channel calculations were performed with the code CCFULL [22] which takes into account the effects of nonlinear coupling to all orders. The calculations used the same nuclear potential

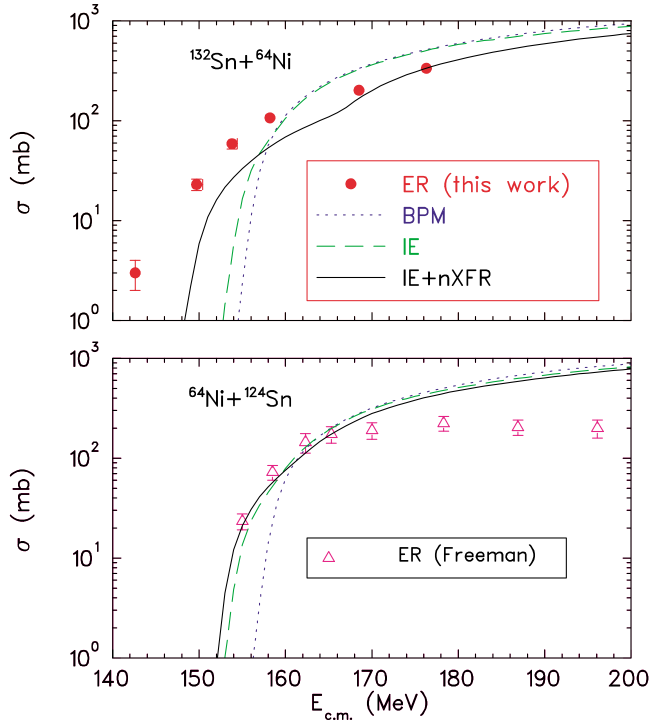

FIG. 3 (color online). Comparison of measured ER excitation functions with fusion model calculations. It is noted that since the fission cross sections are calculated to be negligible at $E_{c.m.} \leq 160$ MeV, the ER cross sections are taken as fusion cross sections. The upper panel is for ^{132}Sn + ^{64}Ni and the lower panel is for ^{64}Ni + ^{124}Sn [15]. The measured ER cross sections are shown by the filled circles and open triangles for ^{132}Sn + ^{64}Ni and ^{64}Ni + ^{124}Sn, respectively. The one-dimensional barrier penetration model (BPM) prediction is shown by the dotted curve. The dashed and solid curves are results of coupled-channel calculations including inelastic excitation (IE), and IE and neutron transfer (nXFR), respectively.

as that for the BPM calculation. The dashed curves in Fig. 3 are the result of coupling to inelastic excitation (IE) of the projectile and target. Table I lists the states and parameters [23,24] for the calculations. As shown in the lower panel of Fig. 3, the calculation reproduces the ^{64}Ni + ^{124}Sn cross sections fairly well at low energies. For ^{132}Sn + ^{64}Ni, the calculation significantly underpredicts the sub-barrier cross sections as shown in the upper panel of Fig. 3. The small effect of coupling to IE in ^{132}Sn can be attributed to the high excitation energy of the 2^+

TABLE I. Parameters used in coupled-channel calculations. λ^π is the spin and parity, and β_λ is the deformation parameter.

Nucleus	λ^π	E^* (MeV)	β_λ
^{64}Ni	2^+	1.346	0.179
^{124}Sn	2^+	1.132	0.095
	3^-	2.614	0.136
^{132}Sn	2^+	4.041	0.06

excited state and the small reduced transition probability [$B(E2)$].

In ^{64}Ni + ^{124}Sn, the (^{64}Ni, ^{66}Ni) reaction is the only transfer channel which has a positive Q value. Coupled-channel calculations including this channel with an empirically determined coupling constant of 0.25 MeV and IE are in good agreement with the fusion cross sections near and below the barrier, as can be seen by the solid curve in the lower panel of Fig. 3. It is noted that the code CCFULL is suitable for reactions where multinucleon transfer is less important than IE [22] as is the case in ^{64}Ni + ^{124}Sn. For the ^{132}Sn-induced reaction, the Q values are positive for ^{64}Ni picking up two to six neutrons which suggests that the observed fusion enhancement may be attributed to multinucleon transfer similar to that observed in ^{40}Ca + ^{96}Zr [25]. Although CCFULL is not expected to treat the coupling of multinucleon transfer accurately, exploratory calculations were carried out to provide a preliminary estimate of the effects of coupling to these channels. Results of calculations including IE and these transfer channels using the same coupling constant as in ^{64}Ni + ^{124}Sn and assuming clusters of neutrons transferred to the ground state are shown by the solid curve in the upper panel of Fig. 3. The calculation cannot account for the cross sections near and below the barrier, nevertheless, it illustrates qualitatively the enhancement of sub-barrier fusion due to the coupling to multinucleon transfer. More realistic calculations which also consider sequential transfer, as pointed out in Ref. [25], may account for the discrepancy. It would be interesting to study near-barrier fusion further using even more neutron-rich Sn isotopes. However, this will be a very challenging task because the present beam intensity for ^{134}Sn at HRIBF is approximately 2000 pps and highly contaminated. On the other hand, HRIBF can provide other pure neutron-rich radioactive beams such as Br and I with reasonable intensities for further studies.

In the future, it is necessary to measure fission for ^{132}Sn + ^{64}Ni in order to obtain the fusion cross sections and study the survival probability of the compound nucleus. In addition, it was found that the extra-push energy [26] is needed for compound nucleus formation in ^{64}Ni on stable even Sn isotopes at high energies [17] and the extra-push energy diminishes as the number of neutrons in Sn increases. The threshold for requiring the extra-push energy given in Ref. [17] is near the ^{132}Sn + ^{64}Ni system. This can be investigated by measuring ER and fission cross sections at higher energies.

In summary, fusion-evaporation cross sections using neutron-rich ^{132}Sn beams on a ^{64}Ni target were measured at energies near the Coulomb barrier. Large sub-barrier fusion enhancement using neutron-rich radioactive heavy ion beams was observed in this experiment. The enhancement cannot be explained by a simple shift of the barrier height, or by the coupling to inelastic excitation channels. There are five neutron transfer channels which have large positive Q values. These reaction channels may serve as doorway states to fusion. Further experiments using neutron-rich radioactive beams would advance our understanding of the mechanism for the fusion enhancement and provide valuable information for using such beams to produce superheavy elements at future radioactive beam facilities.

We wish to thank the HRIBF staff for providing excellent radioactive beams and technical support. We wish to thank S. Novotny for his help with the apparatus. Research at the Oak Ridge National Laboratory is supported by the U.S. Department of Energy under Contract No. DE-AC05-00OR22725 with UT-Battelle, LLC. W. L. and D. P. are supported by the U.S. Department of Energy under Grant No. DE-FG06-97ER41026.

[1] M. Beckerman, Rep. Prog. Phys. **51**, 1047 (1988).
[2] N. Takigawa, H. Sagawa, and T. Shinozuka, Nucl. Phys. **A538**, 221c (1992).
[3] M. S. Hussein, Nucl. Phys. **A531**, 192 (1991).
[4] C. H. Dasso and R. Donangelo, Phys. Lett. B **276**, 1 (1992).
[5] V. Yu. Denisov, Eur. Phys. J. A **7**, 87 (2000).
[6] S. Hofmann, Prog. Part. Nucl. Phys. **46**, 293 (2001).
[7] K. E. Zyromski *et al.*, Phys. Rev. C **55**, R562 (1997).
[8] C. Signorini, Nucl. Phys. **A693**, 190 (2001).
[9] S. Hofmann and G. Münzenberg, Rev. Mod. Phys. **72**, 733 (2000).
[10] D. W. Stracener, Nucl. Instrum. Methods Phys. Res., Sect. B **204**, 42 (2003).
[11] D. Shapira, Nucl. Instrum. Methods Phys. Res., Sect. B **204**, 544 (2003).
[12] D. Shapira *et al.* (to be published).
[13] A. Gavron, Phys. Rev. C **21**, 230 (1980).
[14] J. B. Marion and B. A. Zimmerman, Nucl. Instrum. Methods **51**, 93 (1967).
[15] W. S. Freeman *et al.*, Phys. Rev. Lett. **50**, 1563 (1983).
[16] R. Bass, Nucl. Phys. **A231**, 45 (1974).
[17] K. T. Lesko *et al.*, Phys. Rev. C **34**, 2155 (1986).
[18] A. J. Sierk, Phys. Rev. C **33**, 2039 (1986).
[19] N. Rowley, G. R. Satchler, and P. H. Stelson, Phys. Lett. B **254**, 25 (1991).
[20] M. Dasgupta, D. J. Hinde, N. Rowley, and A. M. Stefanini, Annu. Rev. Nucl. Part. Sci. **48**, 401 (1998).
[21] A. B. Balantekin and N. Takigawa, Rev. Mod. Phys. **70**, 77 (1998).
[22] K. Hagino, N. Rowley, and A. T. Kruppa, Comput. Phys. Commun. **123**, 143 (1999).
[23] S. Raman *et al.*, At. Data Nucl. Data Tables **36**, 1 (1987).
[24] R. H. Spear, At. Data Nucl. Data Tables **42**, 55 (1989).
[25] H. Timmers *et al.*, Nucl. Phys. **A633**, 421 (1998).
[26] W. J. Swiatecki, Phys. Scr. **24**, 113 (1981).